Fitting a Stochastic Model for Golden-Ten

de Vos, J.C.; van der Genugten, B.B.

Publication date:
1996

Fitting a stochastic model for Golden-Ten

J.C. de Vos * B.B. van der Genugten **

Abstract

Golden-Ten is an observation game in which players try to predict the outcome of the motion of a ball rolling down the surface of a drum. This paper describes the motion of the ball as a stochastic model, based on a deterministic, mechanical model. To this end, the motion is split into several stages, each one of which has its own characteristics. The aim of this paper is to construct a simulation model that completely matches the experimental data obtained from earlier research. Even the peculiarities of the special experimental setup will be incorporated. The simulation program is written in MATLAB.

Keywords & phrases Brownian motion, game of chance, game of skill, simulation model, stochastic differential equations.

*Co-operation Centre Tilburg and Eindhoven Universities, P.O. box 90153, 5000 LE Tilburg, The Netherlands

**Tilburg University, Department of Economics, P.O. box 90153, 5000 LE Tilburg, The Netherlands

1 Introduction

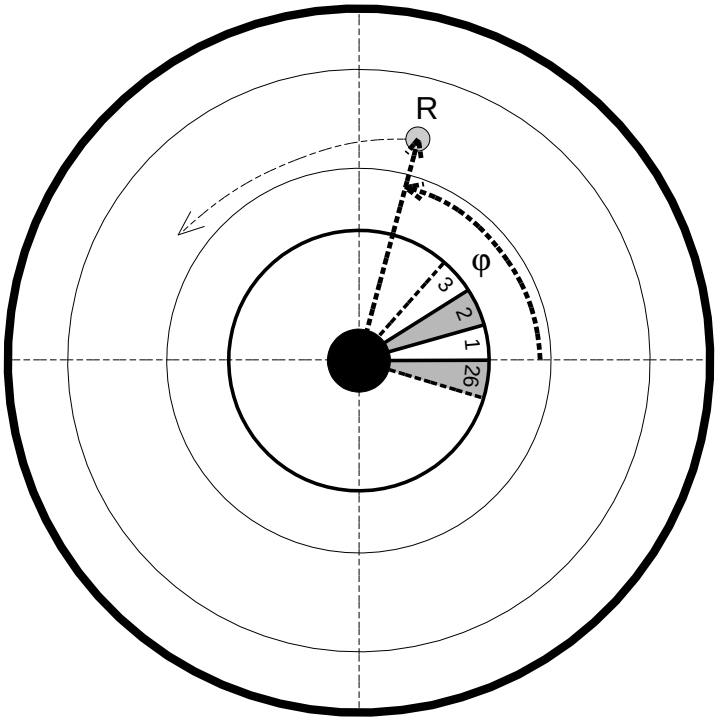

Figure 1: The Golden-Ten drum; top-view.

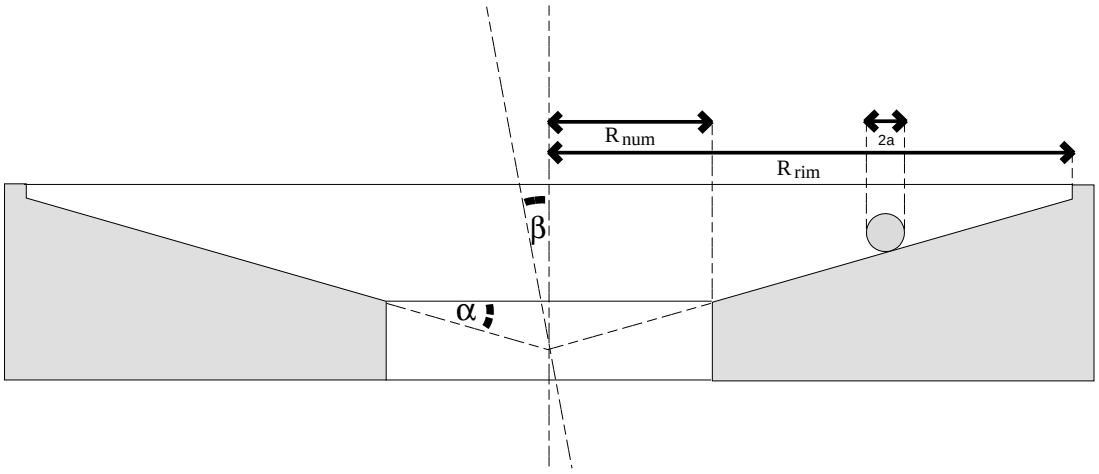

Figure 2: The Golden-Ten drum; side-view.

R_{rim}	R_{obs}	R_{lim}	R_{num}
0.4870	0.390	0.260	0.2050
a	α	β	φ_β
0.0175	0.0831	0.000409	3.6633

Table 1: Physical dimensions of the Golden-Ten attributes (in SI units).

Golden-Ten is an observation game in which players try to predict the outcome of the motion of a ball. This relatively small ball descends in a large drum, and eventually falls down into a numbered ring of twenty-six, equally large compartments, thereby defining the outcome. There is some resemblence with Roulette, albeit that the motion of the Golden-Ten ball is not disturbed by any obstacles on the way. [De Vos] reports the experimental design and the observed orbits of a concrete experiment, whereas [Van de Ven] describes the analytical properties of the equations of motion of the ball in the drum, based on the principal laws of mechanics. Such a deterministic model does however not fit to the experimental data, due to apparent disturbances of a random nature. In this paper we describe the construction of a stochastic model that fits the data. In a forthcoming paper, we will use this stochastic model to derive optimal prediction strategies for players, together with their gains in the long run.

In order to keep this paper self-contained, we here repeat some features of the game. The main attributes are a solid little ball, made of ivory-like synthetic material, and a big - slightly grooved - usually uncoated metal drum. Figures 1 and 2, respectively, show a top- and a side-view of this drum (in figure 2, angle β denotes the slightly tilted position, see [Dissertation]). At the beginning of the game, the ball is launched from a slit plastic arm at the upper rim of the drum. After rolling a few rounds alongside of the rim, the ball gradually spirals down the drum, towards the compartment ring. As with Roulette, the players can bet on one or more possible outcomes, which are represented by the numbers of the compartments. The physical dimensions of our experiment (see [De Vos]) are listed in table 1 (where φ_β denotes the maximum tilt angle).

Because of the smooth surface of the drum, one might expect that the orbit of the ball (from launch upto and including the downfall) is deterministic, which would continuously yield the same outcome. The experimental data in [De Vos] however show an almost uniform distribution of outcomes. This is illustrated in figure 3, which presents the frequencies of 338 arbitrary orbits (i.e. the ones that were readily available). The figure shows neither extremely high nor extremely low levels, and does not show any clear structure. This would imply that the odds in Golden-Ten are basically the same as those in Roulette. Considering the rules of the game, there is however one major diference. As shown in figures 1 and 2, there are two concentric circles on the surface of the Golden-Ten drum. The upper circle is called the observation ring and the lower one the limit ring. The players can start betting when the ball reaches the observation ring, and have to end the betting at the limit ring. Hence the players can observe part of the ball's orbit, which could enable them to make a better than

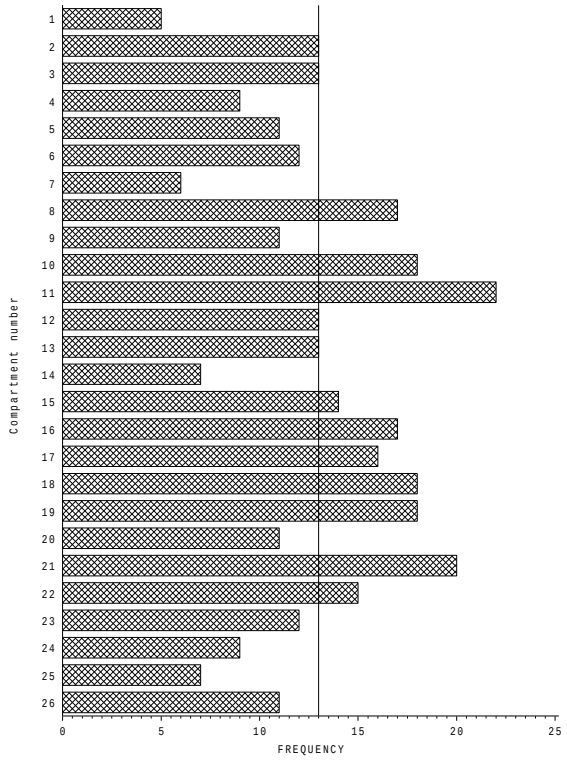

Figure 3: Outcome frequencies.

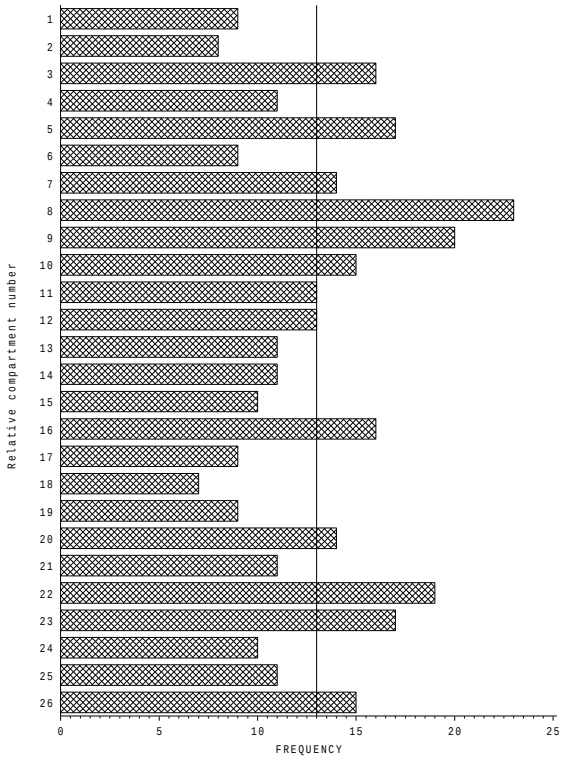

Figure 4: Relative outcome frequencies.

random guess on the outcome. This would suggest that Golden-Ten, unlike Roulette, contains elements of skill.

Figure 4 shows a histogram of the difference in compartment numbers between the limit ring intersection point and the final outcome. The almost uniform distribution indicates that there is no correspondence between those numbers. This implies that a reliable prediction strategy requires much more information. For that reason we firstly present the shortcomings of a deterministic model. Figures 5 to 8 show the main components of such a model, with parameters estimated from a nice, smooth orbit (see [De Vos], orbit T11B21). As opposed to this, figures 9 to 12 present the corresponding components of a common experimental orbit (T11B38, see [De Vos]). This illustrates that the overall characteristics are quite similar - except maybe for the spin (in figures 8 and 12 denoted by $\dot{\psi}$) - but also that the local differences are relatively large. However, small differences may eventually have large effects on the final outcome!

The erratic behaviour shown in figures 10 and 11 may be caused by irregularities on the surface of both drum and ball, or maybe by varying conditions of the surrounding air (due to the ponderous illumination setup used in [De Vos]). They may however also be explained from failing model assumptions in [Van de Ven], such as the one concerning rolling without slipping. Furthermore we know that the surface of the drum in question is slightly grooved. The concentric grooves can cause the ball to get stuck in a kind of trench, as is demonstrated in figure 14, where it apparently

gets stuck in a trench with radius 0.43 (m). Apart from that, the grooves may also account for the odd behaviour of the experimentally determined spin in figure 12 (see also [Dissertation]). This type of peculiarities has to be taken into account, because they will eventually - albeit slightly - influence the final outcome.

The aim of this report is to construct a complete stochastic model that fits the experimental data. In order to grasp the main effects, we start off on a discussion of the deterministic model. The parameters in this model will be estimated from the experimental data. Since the estimates can differ from experiment to experiment, we consequently use the smooth orbit T11B21 (see figure 13) for the particular estimates, and the rest of the experiments to get a rough impression of the range. This deterministic model is described in section 2. The next step will be the extension of this model to a basic stochastic model for a general Golden-Ten setup without any peculiarities (see section 3). Finally, the model will be extended with some particular factors related to the special experimental setup in [De Vos]. We will conclude this report with the first simulation results (in appendix A), and a listing of the full simulation program, written in the MATLAB programming language (appendix B).

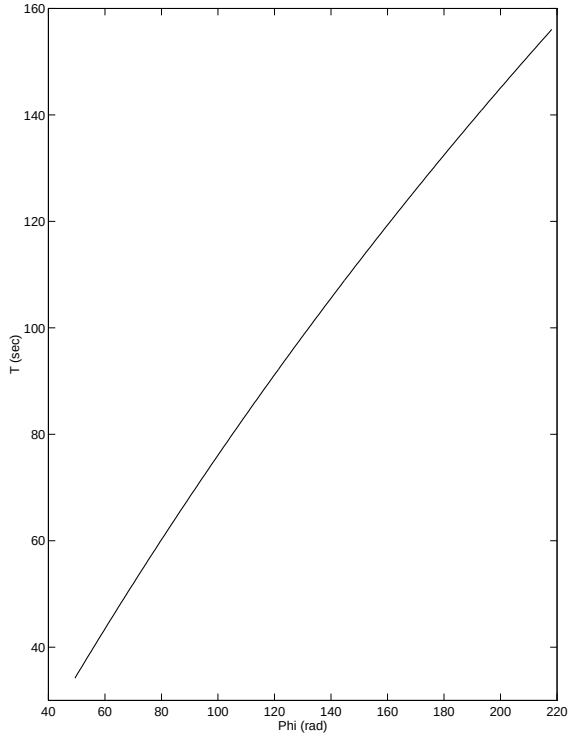

Figure 5: Theoretical, deterministic time.

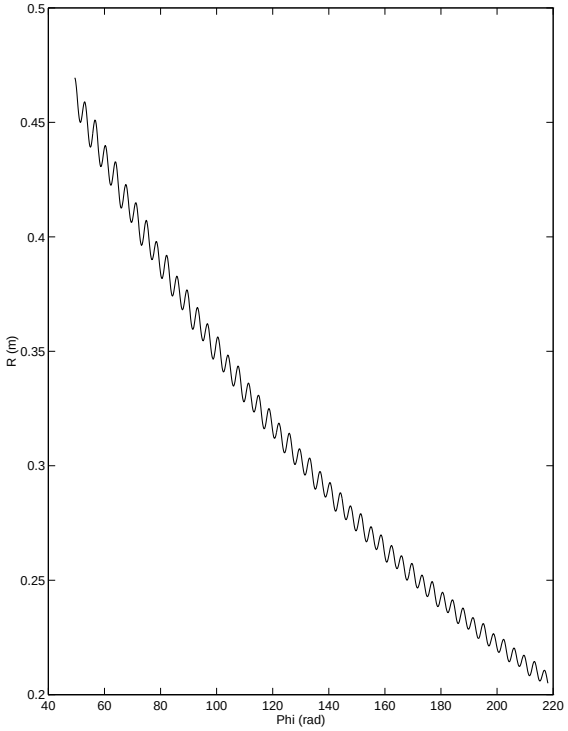

Figure 6: Theoretical radius.

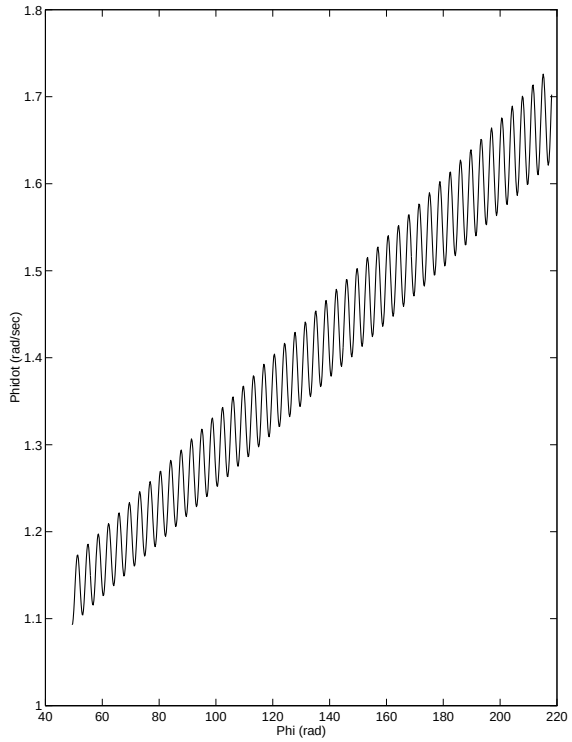

Figure 7: Theoretical angular velocity.

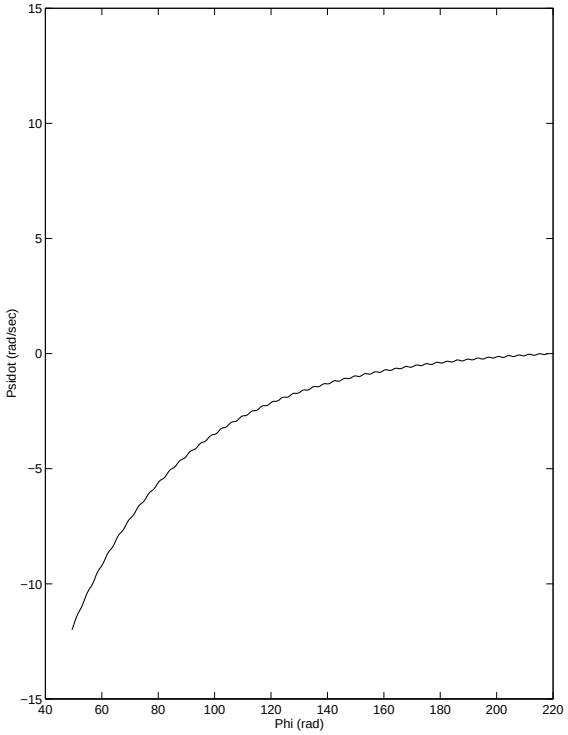

Figure 8: Theoretical spin.

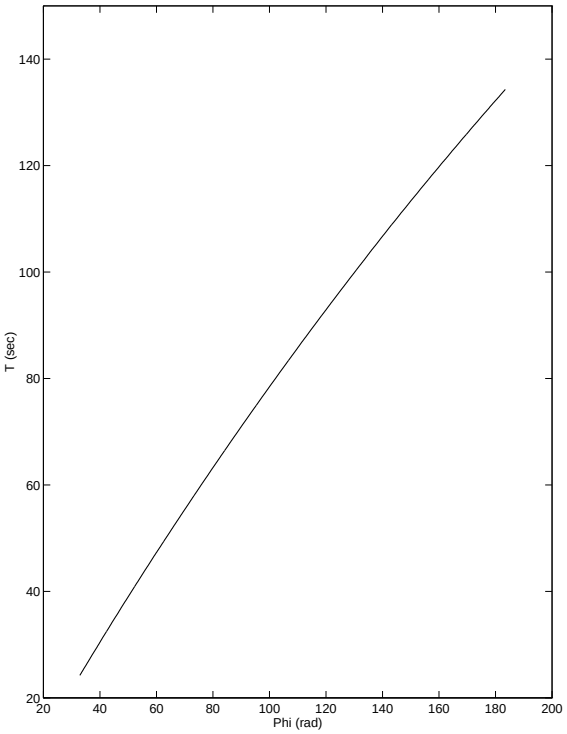

Figure 9: Observed Time.

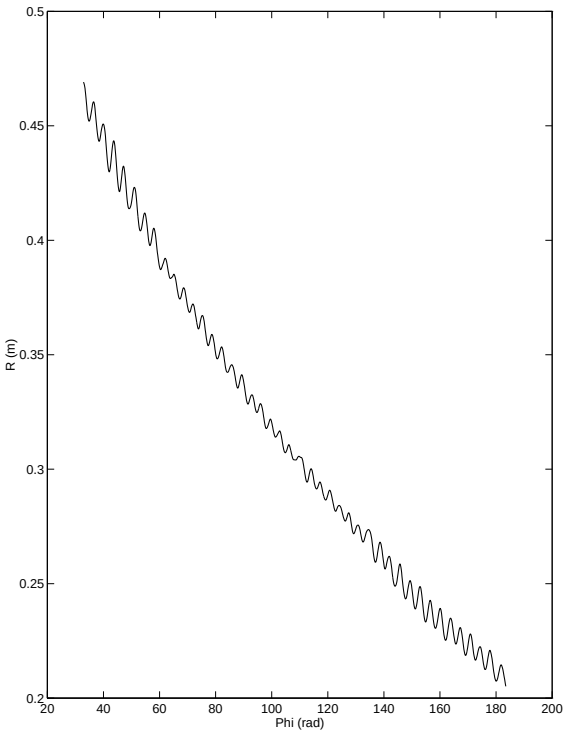

Figure 10: Observed radius.

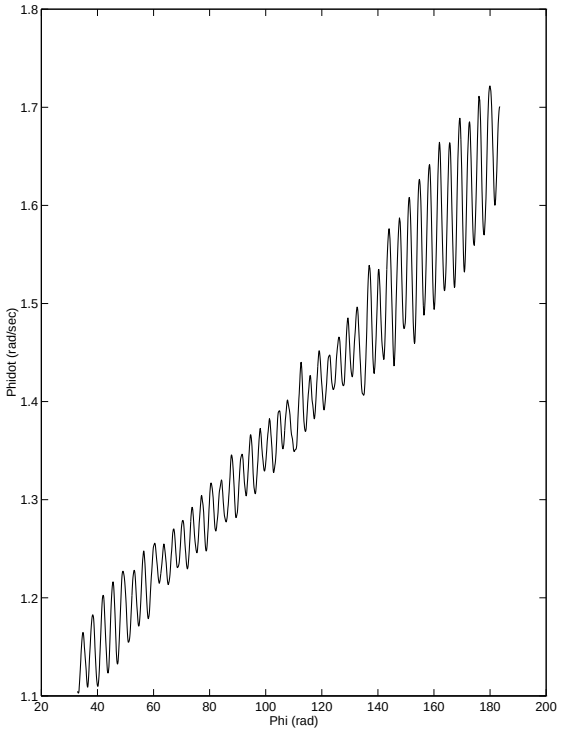

Figure 11: Observed angular velocity.

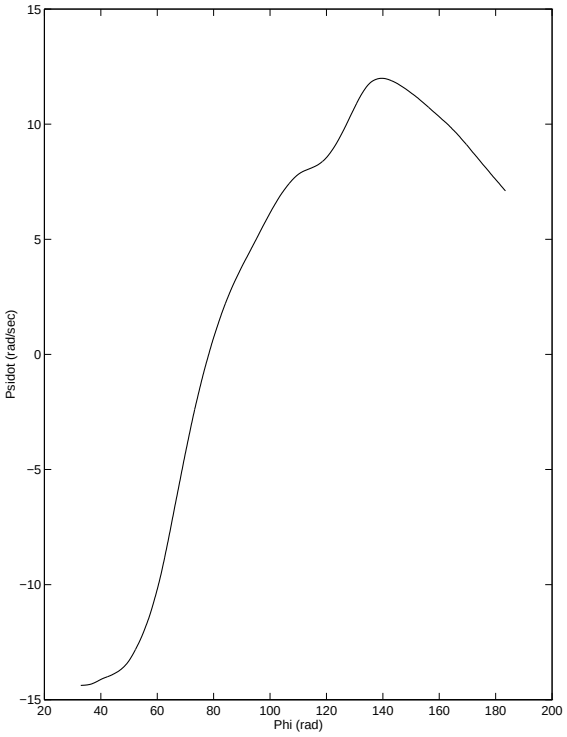

Figure 12: Observed spin (all T11B38).

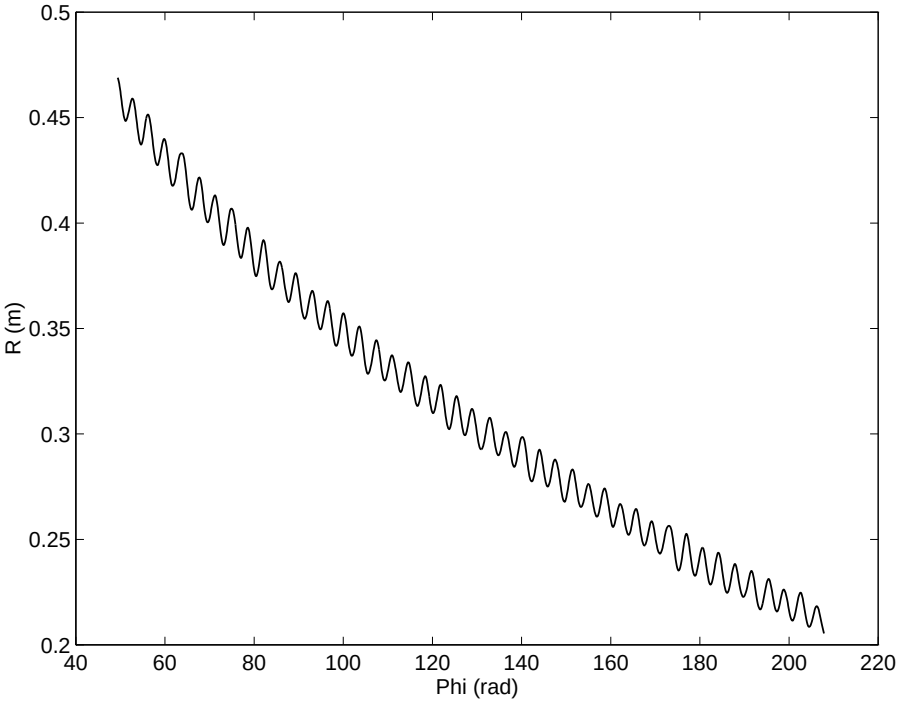

Figure 13: The smooth orbit T11B21.

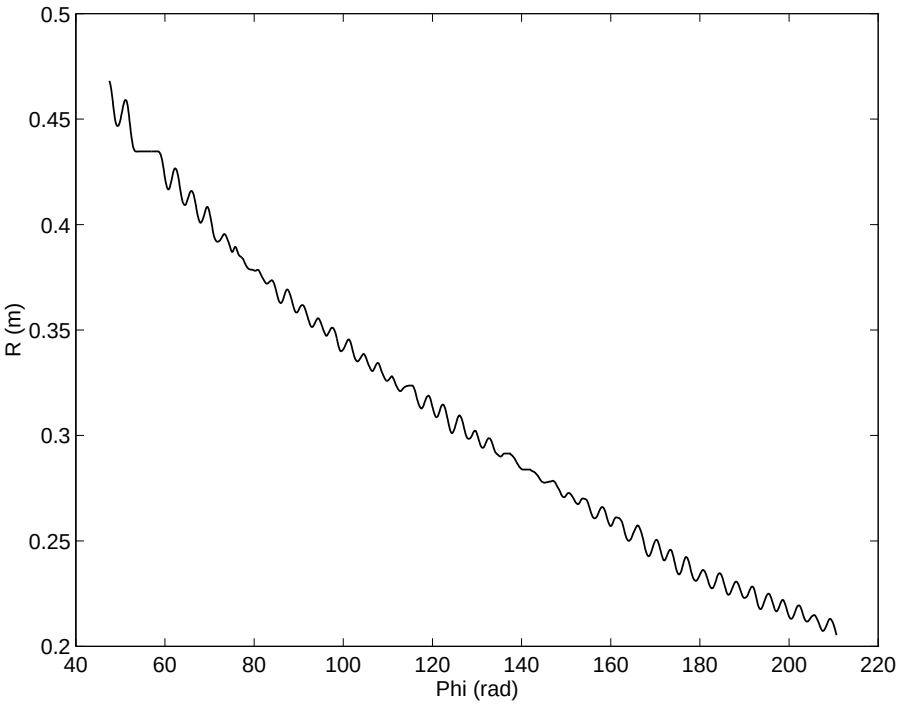

Figure 14: The trenched orbit T11B03.

2 The deterministic model

The total motion consists of three basic stages, each one of which can be subdivided into one or more smaller stages. Each small stage is given an index, ranging from 0 to $n+1$. The same index is given to the starting time of the corresponding stage, as well as to the corresponding initial conditions. Index 0 thus indicates the stage where the ball rolls along the rim, after the launch, and stage 1 is the part where the ball leaves the rim, but still moves in a circular orbit. We call this stage the first trench, although it does not neccessarily have to be caused by the presence of surface grooves; it merely expresses the fact that the ball usually slips along the rim for some time, before it actually starts to descend.

When it comes out of the first trench, the ball rolls down over the surface until radius R reaches a local minimum. The stages where the ball moves between two local extrema are numbered as 2 to $n-1$. Some of these stages can represent a trench motion. The last but one stage - from the last extremum to the edge of the drum - has index n, and the last stage - where the balls falls off of the edge into the numbered ring - has index $n+1$. The final conditions of the last stage are indicated with index $n+2$. We denote the duration of the i^{th} stage as

$$\tau_i = t_{i+1} - t_i,\ i \in \{0, 1, ..., n+1\}. \tag{1}$$

2.1 Rolling along the rim

While the ball is rolling along the rim, the radius R is constantly given by

$$R = R_{rim} - a. \tag{2}$$

When the ball is launched from the slit plastic arm onto the surface, it will - at least for some time - slip along the rim. We assume that after two or three revolutions along the rim the slipping has ended, and we start observing the game at the beginning of stage 0: when the ball passes the compartment lamella between the numbers 26 and 1 for the third time. The observed initial conditions are

$$\begin{array}{lll} t_0 = 0\ (sec) & , & \dot{\psi}_0 = -46\ (rad/sec), \\ R_0 = 0.4695\ (m) & , & \dot{R}_0 = 0\ (m/sec), \\ \varphi_0 = 0\ (rad) & , & \dot{\varphi}_0 = 1.877\ (rad/sec). \end{array} \tag{3}$$

The initial angular velocity does not necessarily have to be fixed, but according to the rules of the game its value lies somewhere in the interval $(1.63, 2.14)\ \ (rad/sec)$ (see also subsection 3.1).

During stage 0, on $[t_0, t_1)$, the motion of the ball is determined by the system

$$\begin{aligned} \ddot{R} &= \dot{R} = 0, \\ R\ddot{\varphi} &= -f_r R\dot{\varphi} + g_r \sin\beta \sin(\varphi - \varphi_\beta), \\ a\dot{\psi} &= -\tfrac{1-\sin\alpha}{\cos\alpha} R\dot{\varphi}, \end{aligned} \tag{4}$$

where f_r denotes a friction coefficient and g_r represents the contribution by gravity:

$$g_r = \frac{5\cos^2\alpha}{7\cos^2\alpha+2(1-\sin\alpha)^2}\, g. \tag{5}$$

The experimental data yield the estimates

$$\begin{array}{rcl} f_r &=& 0.0161 \pm 0.004\ (sec^{-1}), \\ g_r &=& 5.64 \pm 0.01\ (m/sec^2). \end{array} \tag{6}$$

The first stage of the motion ends when the angular velocity reaches the theoretical value

$$\dot\varphi_1 = \sqrt{\frac{5g(\sin\alpha\cos\beta + \cos\alpha\sin\beta\cos(\varphi_1-\varphi_\beta))}{R_1(7\cos\alpha - 2\tan\alpha(1-\sin\alpha))}}, \tag{7}$$

see [Van de Ven]. Use of this condition leads to the final values

$$\begin{array}{lll} t_1 = 31.42\ (sec) & , & \dot\psi_1 = -28\ (rad/sec), \\ R_1 = 0.4695\ (m) & , & \dot R_1 = 0\ (m/sec), \\ \varphi_1 = 46.31\ (rad) & , & \dot\varphi_1 = 1.128\ (rad/sec). \end{array} \tag{8}$$

When the ball leaves the rim, it immediately gets stuck in the so-called first trench. This is stage 2 of the motion, starting from the conditions in (8). On the analogy of system (4), taking $\beta = 0$, we pose the simplified model (on $[t_1, t_2)$)

$$\begin{array}{rcl} R &=& R_1, \\ \varphi &=& \varphi_1 + \frac{1}{f_1}\dot\varphi_1\{1 - e^{-f_1(t-t_1)}\}, \\ \dot\psi &=& \dot\psi_1 e^{-h_1(t-t_1)}, \end{array} \tag{9}$$

where coefficients f_1 and h_1 are estimated as

$$\begin{array}{rcl} f_1 &=& 0.0115 \pm 0.002\ (sec^{-1}), \\ h_1 &=& 0.3 \pm 0.2\ (sec^{-1}). \end{array} \tag{10}$$

The final conditions, obtained from the experimental data, are

$$\begin{array}{lll} t_2 = 34.32\ (sec) & , & \dot\psi_2 = -12\ (rad/sec), \\ R_2 = 0.4695\ (m) & , & \dot R_2 = 0\ (m/sec), \\ \varphi_2 = 49.50\ (rad) & , & \dot\varphi_2 = 1.093\ (rad/sec). \end{array} \tag{11}$$

These values strongly depend on the actual value of $\dot\varphi_0$ in (3). Due to possible variation, the final angle φ may range from 35 to 65 (rad), and the final time from 25 to 40 (sec). Furthermore we have observed a strong influence, especially on final angular velocity $\dot\varphi_2$, of the actual size of trench time τ_1. The time range of $(0, 4)$ (sec) induces a typical range for $\dot\varphi_2$ of $(1.07, 1.13)$ (rad/sec) (see also subsection 3.1).

2.2 Rolling on the surface

After leaving the trench along the rim, the ball starts rolling on the surface. The equations of motion on $[t_2, t_{n+1})$ are (see [Van de Ven])

$$\begin{aligned} \ddot{R}/\cos\alpha &= -\tfrac{5}{7}f\dot{R}\cos\alpha + R\dot{\varphi}^2\cos\alpha + \tfrac{2}{7}a\dot{\varphi}\dot{\psi}\sin\alpha \\ &\quad -\tfrac{5}{7}g(\sin\alpha\cos\beta + \cos\alpha\sin\beta\cos(\varphi-\varphi_\beta)), \\ R\ddot{\varphi} &= -\tfrac{5}{7}fR\dot{\varphi} - 2\dot{R}\dot{\varphi} + \tfrac{5}{7}g\sin\beta\sin(\varphi-\varphi_\beta), \\ a\ddot{\psi} &= -ha\dot{\psi} - \dot{R}\dot{\varphi}\tan\alpha, \end{aligned} \tag{12}$$

where f represents an air friction coefficient, and h a spin friction coefficient. Anticipating on the stochastic model in section 3, we have redimensioned the equations in [Van de Ven] such that all factors in the system represent forces (setting aside the constant mass m). The coefficients in (12) are estimated from the experimental data as

$$\begin{aligned} f &= 0.0139 \pm 0.003\ (sec^{-1}), \\ h &= 0.027 \pm 0.02\ (sec^{-1}). \end{aligned} \tag{13}$$

Since we are considering a deterministic model, we assume that the ball does not get stuck into any more trenches. The final conditions of the part where the ball rolls over the surface can therefore be found by numerically solving equation system (12), with initial conditions (11). This yields

$$\begin{aligned} t_{n+1} &= 156.06\ (sec) \quad , \quad \dot{\psi}_{n+1} = 0\ (rad/sec), \\ R_{n+1} &= 0.2050\ (m) \quad , \quad \dot{R}_{n+1} = -0.0098\ (m/sec), \\ \varphi_{n+1} &= 218.12\ (rad) \quad , \quad \dot{\varphi}_{n+1} = 1.70\ (rad/sec), \end{aligned} \tag{14}$$

and, according to figure 6,

$$n = 94. \tag{15}$$

Due to the large variation in the initial conditions (11), and also - albeit to a lesser extent - due to the variation of the coefficients in (6), (10) and (13), the final conditions in (14) may vary enormously. The experimental data show a typical range for n of $(65, 110)$, for t_{n+1} of $(120, 170)$ (sec), and for φ_{n+1} of $(160, 240)$ (rad).

2.3 Falling down into the ring

The final part of the ball's motion is rather capricious, since the ball may or may not for some time roll or slip along the drum's edge, and furthermore it may bounce on one or more partition lamellae before it actually comes down in the final compartment. All we actually have observed is that the difference between the compartment number where the ball leaves the surface, and the game's final outcome, varies from 0 to 3 (modulo 26). We can express the expected relation (operative on $[t_{n+1}, t_{n+2}]$) as

$$\varphi_{n+2} = \varphi_{n+1} + \tfrac{3}{26}\pi. \tag{16}$$

The relation between angles and compartment numbers is given by

$$N = 1 + [\tfrac{13}{\pi}\varphi \ mod\ 26]. \tag{17}$$

From the final angle in $(14)^3$, and the extra jump in equation (16), we find the outcome N_{n+2} of our deterministic model to be 21. However, due to the large variation of the angle in $(14)^3$, the strategy to always bet on this particular number is absurd. From the almost uniform distribution in figure 3, we conclude that a deterministic model is simply not appropriate. In the next section we present a better model.

3 The basic stochastic model

3.1 Rolling along the rim

The first stage of the motion starts off with a more or less arbitrary angular velocity $\dot{\varphi}_0$, and ends when velocity $\dot{\varphi}$ reaches the theoretical value $\dot{\varphi}_1$ in (7). During this stage, on $[t_0, t_1)$, the ball moves according to system (4). Under the assumption that $\beta = 0$, the explicit solution for the angular velocity on $[t_0, t_1)$ is

$$\dot{\varphi} = \dot{\varphi}_0 e^{-f_r(t-t_0)}. \tag{18}$$

According to the rules of the game, the ball should complete five to ten rounds before it leaves the rim. This implies

$$\dot{\varphi}_0 \in \dot{\varphi}_1 + f_r(10\pi, 20\pi). \tag{19}$$

At time t_1 we have $\dot{\varphi}_1 = 1.127\ (rad/sec)$, wherefore we take

$$\dot{\varphi}_0 \sim U(1.63, 2.14)\ (rad/sec). \tag{20}$$

The actual value of $\dot{\varphi}_0$ in (20) together with the final value $\dot{\varphi}_1$ in (7), determines the final conditions for stage 0. These are in turn the initial conditions for stage 1. For the duration of this stage (from t_1 to t_2) we pose

$$\tau_1 = 1.476 + \eta_1\ (sec), \tag{21}$$

where η_1 is randomly sampled from the distribution in table 2, with $k = 1$.

t	.	.	.	.	-1.476	-1.350	-1.050	-0.750	-0.450	-0.150
$P(\eta_k \leq t)$	.	.	.	.	0.000	0.017	0.054	0.131	0.330	0.576
t	0.150	0.450	0.750	1.050	1.350	1.650	1.950	2.250	2.550	2.850
$P(\eta_k \leq t)$	0.713	0.840	0.913	0.955	0.978	0.990	0.994	0.998	0.999	1.000

Table 2: Cumulative distribution of corrected trench times.

3.2 Rolling on the surface

The motion of the ball on the surface is influenced by a conglomerate of small, random forces and moments. This can be modelled by transforming the equations of motion (12) on $[t_2, t_{n+1})$ into the system of stochastic differential equations

$$\begin{aligned} \ddot{R}/\cos\alpha &= -\tfrac{5}{7}f\dot{R}\cos\alpha + R\dot{\varphi}^2\cos\alpha + \tfrac{2}{7}a\dot{\varphi}\dot{\psi}\sin\alpha \\ &\quad -\tfrac{5}{7}g(\cos\alpha\sin\beta\cos(\varphi-\varphi_\beta)+\sin\alpha\cos\beta)+\sigma_1\varepsilon_1, \\ R\ddot{\varphi} &= -\tfrac{5}{7}fR\dot{\varphi} - 2\dot{R}\dot{\varphi} + \tfrac{5}{7}g\sin\beta\sin(\varphi-\varphi_\beta)+\sigma_2\varepsilon_2, \\ a\dot{\psi} &= -ha\dot{\psi} - \dot{R}\dot{\varphi}\tan\alpha + \sigma_3\varepsilon_3, \end{aligned} \tag{22}$$

where the integrated $\varepsilon_i = \varepsilon_i(t)$ represent three independent processes of standard Brownian motion (see e.g. [Schuss]). The estimated standard deviations are

$$\begin{aligned} \sigma_1 &= 4.0\times10^{-3}\ (m/sec^2), \\ \sigma_2 &= 2.9\times10^{-3}\ (m/sec^2), \\ \sigma_3 &= 0, \end{aligned} \tag{23}$$

see [Dissertation].

The motion on the surface ends when the ball falls down into the numbered ring, i.e.

$$R_3 = R_{num} = 0.2050\ (m). \tag{24}$$

This determines the final conditions for this stage of the motion, which are the initial conditions for the next one.

3.3 Falling down into the ring

The ball falls down from the surface into the ring at angle φ_{n+1}, which corresponds to compartment number N_{n+1}. Let γ denote the fractional compartment position at the time of the fall:

$$\gamma = \tfrac{13}{\pi}\varphi_{n+1} - [\tfrac{13}{\pi}\varphi_{n+1}]. \tag{25}$$

Furthermore let

$$\nu = min\{3, max\{0, -9.047 + 6.367\dot{\varphi}_{n+1} + 1.158\gamma + \sigma_\nu Z\}\}, \tag{26}$$

with

$$\sigma_\nu = 0.4043, \tag{27}$$

where Z follows the standard normal distribution $N(0,1)$. The final outcome of the game has thus (c.f. [Dissertation]) been fitted as

$$N_{n+2} = 1 + [(N_{n+1} + \nu - 1)\ mod\ 26]. \tag{28}$$

4 The completed stochastic model

4.1 Rolling through a trench

While moving down the drum, the ball will sometimes get stuck in a local trench. This can happen only when the ball momentarily moves in a circular orbit or - equivalently - when radius R has a local extremum. Because of different local characteristics of the surface, the probability p_i that a trench will occur at stage i depends on the momentary position of the ball, as well as on the nature of the extremum. Since the characteristics of the observation and the limit ring are different from those of the rest of the surface, we composed four probability tables: two for local maxima of R - i.e. one for the rings (table 4) and one for the rest of the surface (table 3) - and likewise two for local minima (tables 6 and 5). These tables give the conditional probabilities

$$p_i = P(R_{i+1} = R_i | sgn(R_i - R_{i-1}), R_i, \varphi_i), \tag{29}$$

for those indices $i \in \{3, 4, ..., n-1\}$ with $sgn(R_i - R_{i-1}) \neq 0$. Note that these probabilities are given per segment, where the rings are divided into 56 segments each, and the rest of the surface into 4×56 segments.

Let K denote the subset of indices that represent a trench, and let $k \in K$. Then the motion during stage k for general k closely resembles that through the trench along the rim, which is in fact the stage with $k = 1$. On the analogy of system (9) we pose on $[t_k, t_{k+1})$:

$$\begin{aligned} R &= R_k, \\ \varphi &= \varphi_k + \tfrac{1}{f_k}\dot{\varphi}_k\{1 - e^{-f_k(t-t_k)}\}, \\ \dot{\psi} &= \dot{\psi}_k e^{-h_k(t-t_k)}, \end{aligned} \tag{30}$$

where

$$\begin{aligned} f_k &= 0.0113 + 0.0017 sgn(R_k - R_{k-1})\ (sec)^{-1} \\ h_k &= 0 \end{aligned} \quad , \ k > 1. \tag{31}$$

For the duration of stage k we take

$$\tau_k = 0.4301 + 1.699 R_k \dot{\varphi}_k - 0.3149\, sgn(R_k - R_{k-1}) + \eta_k\ (sec),\ k > 1, \tag{32}$$

where η_k follows the distribution in table 2. Equations (30) and (32) show that the momentary loss of energy is lower in a minimum than in a maximum, but on the other hand also that the trench time in a minimum is usually longer (see [Dissertation]).

4.2 Rolling freely on the surface

All further extensions to the basic model in section 3 concern the stages where the ball moves over the surface, without rolling through a trench. Let ℓ, with $\ell \notin K$, represent such a stage. The system of stochastic differential equations on $[t_\ell, t_{\ell+1})$

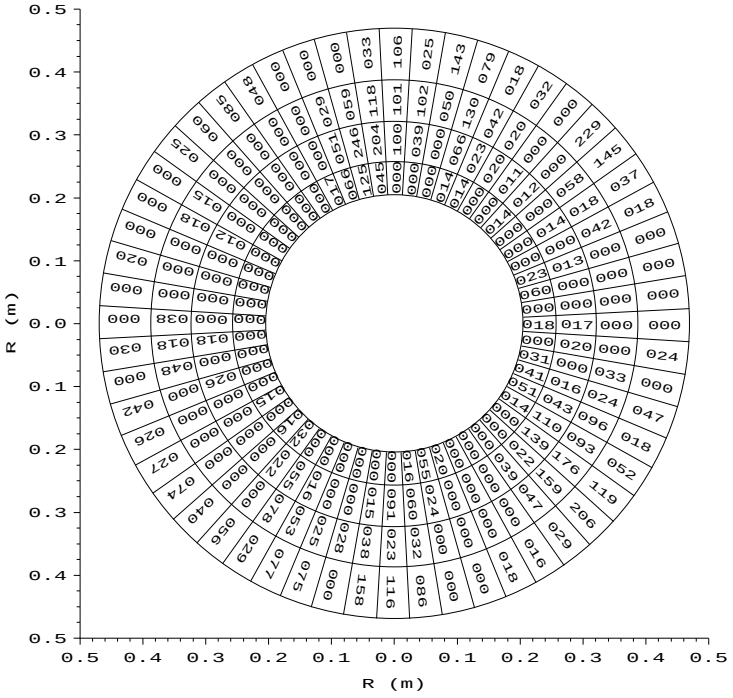

Table 3: Trench probabilities $p_i \times 1000$ for local maxima outside the rings.

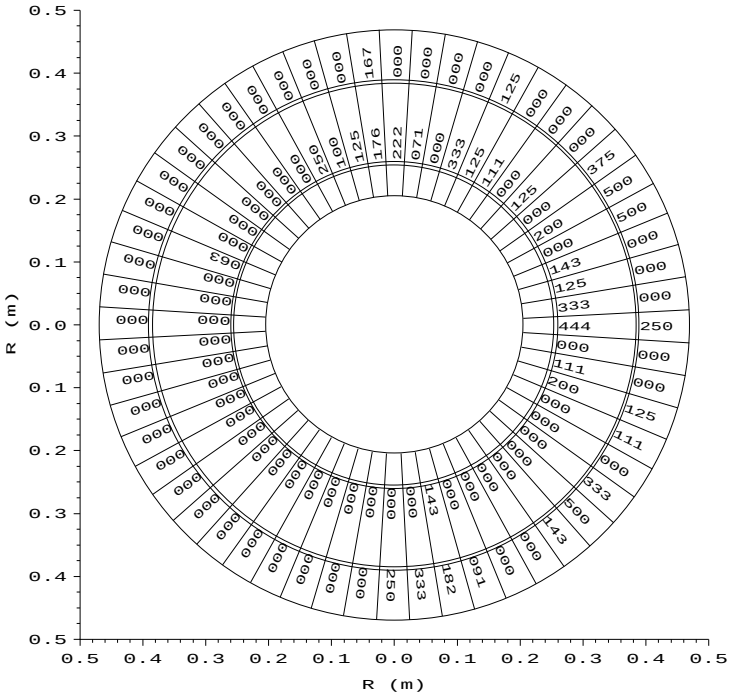

Table 4: Trench probabilities $p_i \times 1000$ for local maxima inside the rings.

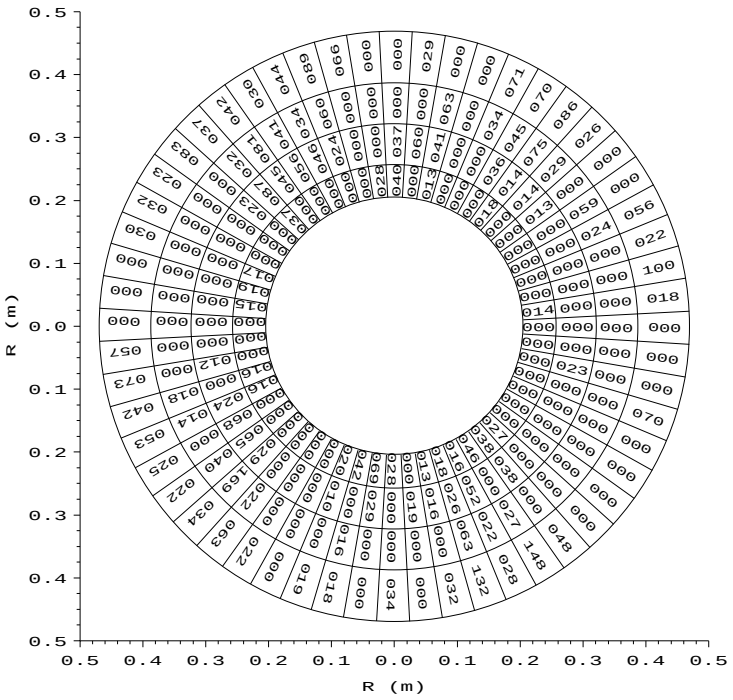

Table 5: Trench probabilities $p_i \times 1000$ for local minima outside the rings.

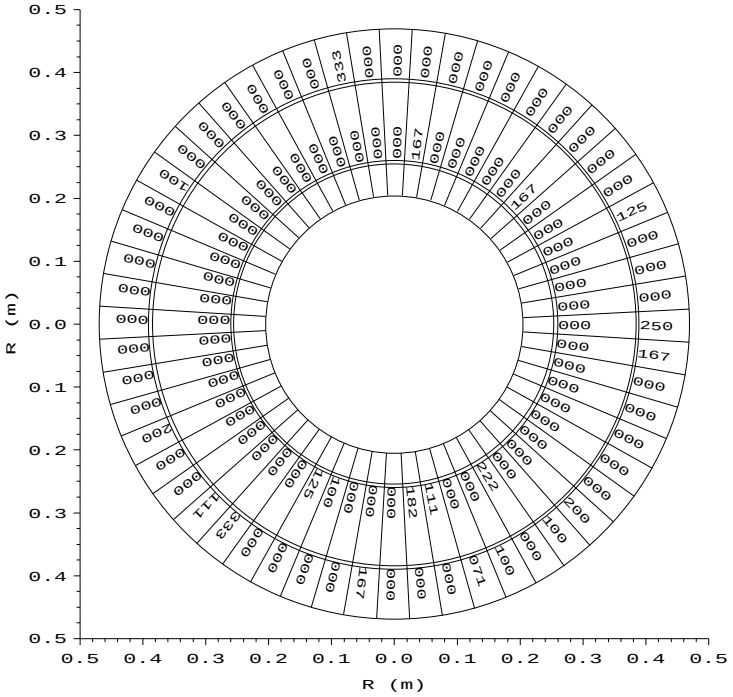

Table 6: Trench probabilities $p_i \times 1000$ for local minima inside the rings.

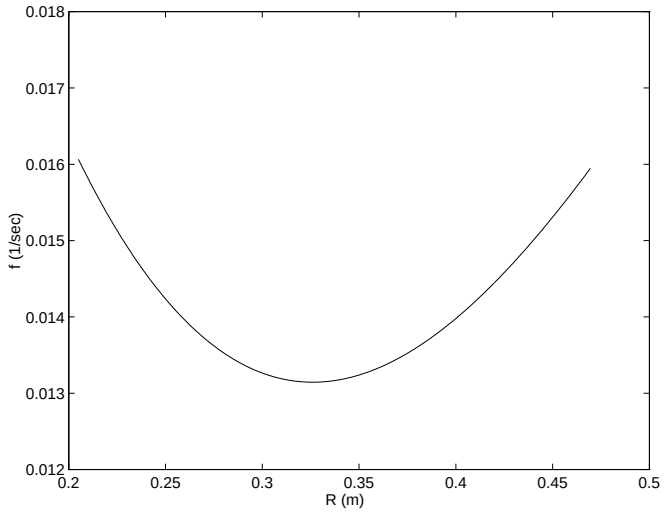

Figure 15: A varying friction coefficient

now changes from (22) into

$$\begin{aligned} \ddot{R}/\cos\alpha &= -\tfrac{5}{7}f(R)\dot{R}\cos\alpha + R\dot{\varphi}^2\cos\alpha + \tfrac{2}{7}a\dot{\varphi}\dot{\psi}\sin\alpha \\ &\quad -\tfrac{5}{7}g(\cos\alpha\sin\beta\cos(\varphi-\varphi_\beta)+\sin\alpha\cos\beta) + \sigma_1\varepsilon_1, \\ R\ddot{\varphi} &= -\tfrac{5}{7}f(R)R\dot{\varphi} - 2\dot{R}\dot{\varphi} + \tfrac{5}{7}g\sin\beta\sin(\varphi-\varphi_\beta) + \sigma_2\varepsilon_2, \\ a\dot{\psi} &= -ha\dot{\psi} + wR\dot{\varphi} - \dot{R}\dot{\varphi}\tan\alpha + \sigma_3\varepsilon_3, \end{aligned} \tag{33}$$

where friction coefficient f has been made R-dependent according to

$$f(R) = -0.2382R^3 + 0.4034R^2 - 0.1871R + 0.03952\ (sec^{-1}), \tag{34}$$

and a winding coefficient w has been added, of estimated size

$$w = 0.0095\ (sec^{-1}). \tag{35}$$

Figure 15 shows that the air resistance near the edges of the drum is relatively large. This phenomenon can be explained from the existence of strong flows of air, caused by the ponderous illumination setup. Coefficient w accounts for the curious behaviour of the spin in figure 12. Presumably due to the existence of surface grooves, the ball experiences a winding moment that eventually causes a sign flip. Note that the final magnitude is determined by the ratio of w and h, the latter of which acts as a brake (see [Dissertation]).

5 Conclusions

Section 4 describes a complete stochastic simulation model, based on the mechanical, deterministic model in [Van de Ven], and fitting the experimental data in [De Vos].

This model is complete in the sense that it deals with a wide variability in environmental conditions, such as a tilted drum, a grooved drum surface, or a varying air friction coefficient. An example of a simulated orbit is given in appendix A, and the corresponding simulaton program in appendix B.

When the game is played under ideal circumstances, i.e. without any of these oddities, we can stick to the basic stochastic model in section 3. In future research we will use the last mentioned model to derive optimal prediction strategies and calculate expected gains. The complete model then serves as an indicator for the success of these strategies under less ideal circumstances. Since both models are very flexible, we can easily adjust the required parameters to fit virtually any imaginable Golden-Ten game site.

A A sample orbit

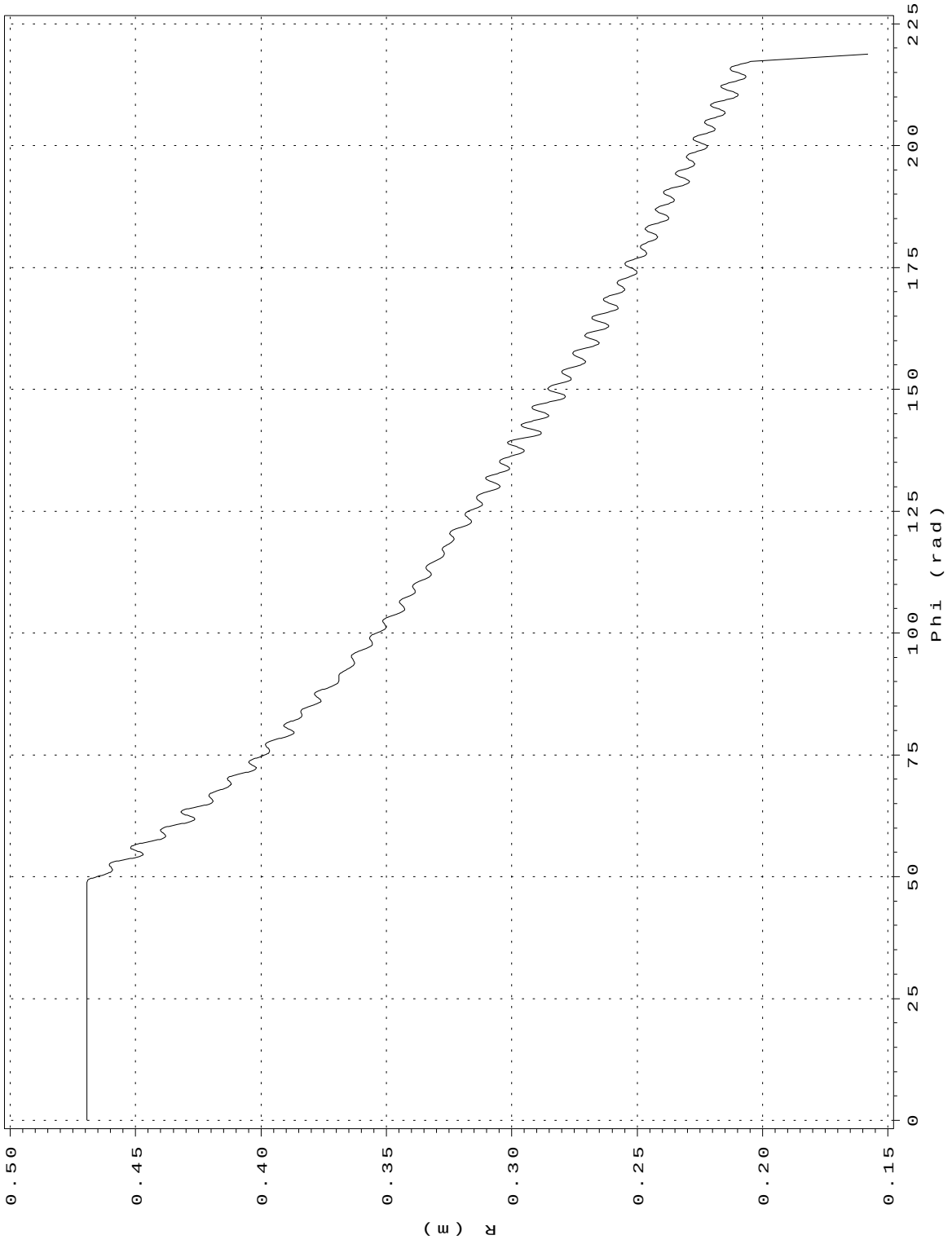

B The simulation program

```
% paper orientation
orient landscape
set(1,'PaperType','A4')

% physical constants
g=9.807;
Rrim=0.487; Rnum=0.205;
Robs=0.390; Rlim=0.260;
dR=0.005; Rmin=0.158;
AA=0.0175; Alpha=0.0831;
Beta=0.000409; Phibeta=3.6633;
global AA Alpha Beta Phibeta

% initial values
r0=Rrim-AA;
Phidot0=sqrt(5*g/r0*sin(Alpha+Beta)/...
            (7*cos(Alpha)-2*tan(Alpha)*(1-sin(Alpha))));
Psidot0=-r0*Phidot0*(1-sin(Alpha))/(A*cos(Alpha));
Spin0=-12;
global Phidot0

% friction coefficients
Fr=0.0161;
F1=0.0115; Ft=0.0113; dF=0.0017;
FR=[-0.2382 0.4034 -0.1871 0.03952];
global Fr FR
HH=0.027; WW=0.0095;
H1=0.3; Hk=0;
global HH WW

% error variables
sigma1=0.0040;
sigma2=0.0029;
sigma3=0;

% trench tables
load surfhigh.tab
load ringhigh.tab
load surflow.tab
load ringlow.tab
load trenchtm.tab

% simulation
```

```
for i=1:350

% along the rim
    phidinit=Phidot0+10*Fr*(1+rand(1))*pi;
    t0=0; x0=[0 phidinit];
    tf=2*log(phidinit/Phidot0)/Fr;
    [t,x]=ode45('rkrim',t0,tf,x0,1e-6);
    nx=find(x(:,2)<Phidot0); nx=nx(1)-1;
    tx=t(nx)+(t(nx+1)-t(nx))*(x(nx,2)-Phidot0)/(x(nx,2)-x(nx+1,2));
    T=[[0:0.08:tx]';tx];
    R=r0*ones(size(T)); Rdot=zeros(size(T));
    Phi=table1([t,x(:,1)],T);
    Phidot=table1([t,x(:,2)],T);
    Psidot=-r0/AA*(1-sin(Alpha))/cos(Alpha)*Phidot;

% through the first trench
    tf=table1([trenchtm(:,2),trenchtm(:,1)],rand(1));
    t=[[0:0.08:tf]';tf];
    n=length(T); T=[T(1:n-1);t];
    R=r0*ones(size(T)); Rdot=zeros(size(T));
    Phi=[Phi(1:n-1);Phi(n)+Phidot0/F1*(1-exp(-F1*t))];
    Phidot=[Phidot(1:n-1);Phidot0*exp(-F1*t)];
    Psidot=[Psidot(1:n-1);Psidot(n)*exp(-H1*t)];

% on the surface
    n=length(T);
    t0=T(n); x0=[R(n) Rdot(n) Phi(n) Phidot(n) Psidot(n)];
    t=t0; x=x0;
    while x0(1)>Rnum
          E1=sigma1*randn(1); E2=sigma2*randn(1);
          [ti,xi]=ode45('rksurf',t0,t0+0.08,x0,1e-6);
          nx=find(abs(diff(sign(xi(:,2))))==2);
          if ~isempty(nx)
             nx=nx(1);
             tx=ti(nx)+(ti(nx+1)-ti(nx))*xi(nx,2)/...
                       (xi(nx,2)-xi(nx+1,2));
             xx=table1([ti,xi],tx);
             si=sign(xi(nx,2));
             if (xx(1)<Robs & xx(1)>Robs-dR) | ...
                (xx(1)<Rlim & xx(1)>Rlim-dR)
                if si>0 then p=table1(ringhigh,xx(3));
                else p=table1(ringlow,xx(3)); end
             else
                if si>0 then p=table1(surfhigh,xx(3));
                else p=table1(surflow,xx(3)); end
```

```
            end
            % through a trench
            if rand(1)<=p
               Fk=Ft+si*dF;
               tf=0.4301+1.699*x0(1)*x0(4)-0.3149*si+...
                  table1([trenchtm(:,2),trenchtm(:,1)],rand(1));
               ti=[[0:0.08:tf]';tf];
               r=xx(1)*ones(size(ti));
               rdot=zeros(size(ti));
               phi=x0(3)+x0(4)/Fk*(1-exp(-Fk*ti));
               phidot=x0(4)*exp(-Fk*ti);
               psidot=x0(5)*exp(-Hk*ti);
               n=length(t); ni=length(ti);
               t=[t(1:n-1);ti];
               x=[x;[r rdot phi phidot psidot]];
               n=length(t);
               ti=t(n); xi=x(n,:);
               t=t(1:n-1); x=x(1:n-1,:);
            end
         end
         ni=length(ti);
         t0=ti(ni); x0=xi(ni,:);
         t=[t;t0]; x=[x;x0];
   end
   n=length(T);
   T=[T(1:n-1);t];
   R=[R(1:n-1);x(:,1)]; Rdot=[Rdot(1:n-1);x(:,2)];
   Phi=[Phi(1:n-1);x(:,3)]; Phidot=[Phidot(1:n-1);x(:,4)];
   Psidot=[Psidot(1:n-1);x(:,5)];

% down to the numbered ring
   n=length(T);
   Nf=1+fix(rem(13*Phi(n)/pi,26));
   C=rem(13*Phi(n)/pi,1);
   dN=min(3,max(0,...
   round(-9.547+6.367*Phidot(n)+1.158*C+0.4043*randn(1))));
   Nf=1+fix(rem(Nf+dN-1,26));
   Phif=Phi(n)+(dN+(0.5-C))*pi/13;
   tf=(Phif-Phi(n))/Phidot(n);
   a=-2*(AA+Rdot(n)*tf)/(tf^2);
   t=[[0:0.08:tf]';tf];
   T=[T(1:n-1);T(n)+t];
   R=[R(1:n-1);R(n)+Rdot(n)*t+0.5*a*t.^2];
   Rdot=[Rdot(1:n-1);Rdot(n)+a*t];
   Phi=[Phi(1:n-1);Phi(n)+Phidot(n)*t];
```

```
    Phidot=[Phidot(1:n-1);Phidot(n)*ones(size(t))];
    Psidot=[Psidot(1:n-1);Psidot(n)*((dt-t)/dt)];
    n=length(T);
    tf=0.0845;
    T=[T;T(n)+tf];
    R=[R;R(n)+Rdot(n)*tf+0.5*a*tf^2]; Rdot=[Rdot;Rdot(n)+a*tf];
    Phi=[Phi;Phi(n)]; Phidot=[Phidot;0]; Psidot=[Psidot;0];

% on the numbered ring
    n=length(T);
    tf=(-Rdot(n)+sqrt(Rdot(n)^2-2*a*Rmin))/a;
    t=[[0:0.08:tf]';tf];
    T=[T(1:n-1);T(n)+t];
    R=[R(1:n-1);R(n)+Rdot(n)*t+0.5*a*t.^2];
    Rdot=[Rdot(1:n-1);Rdot(n)+a*t];
    Phi=[Phi(1:n-1);Phi(n)*ones(size(t))];
    Phidot=[Phidot(1:n-1);Phidot(n)*zeros(size(t))];
    Psidot=[Psidot(1:n-1);Psidot(n)*zeros(size(t))];
    n=length(T);
    tf=0.08;
    T=[T;T(n)+tf]; R=[R;R(n)]; Rdot=[Rdot;0];
    Phi=[Phi;Phi(n)]; Phidot=[Phidot;0]; Psidot=[Psidot;0];

end
```

References

[De Vos] J.C. de Vos, A thousand Golden-Ten orbits. *Report FEW 654*, Tilburg University (1994), 80 pp.

[Dissertation] J.C. de Vos, *Golden-Ten and other trajectory games.* Dissertation at Tilburg University, to appear in 1997.

[Van de Ven] J.C. de Vos and A.A.F. van de Ven, The Golden-Ten equations of motion. To appear in: *Journal of Engineering Mathematics* (1996), 26 pp.

[Schuss] Z. Schuss, *Theory and applications of stochastic differential equations.* New York: John Wiley & Sons (1980), 321 pp.